Journal of Photochemistry and Photobiology B: Biology 92 (2008) 165–174

Contents lists available at ScienceDirect

Journal of Photochemistry and Photobiology B: Biology

journal homepage: www.elsevier.com/locate/jphotobiol

Toward understanding the high PDT efficacy of chlorin e6–polyvinylpyrrolidone formulations: Photophysical and molecular aspects of photosensitizer–polymer interaction *in vitro*

H.A. Isakau [a,1], M.V. Parkhats [b,1], V.N. Knyukshto [b], B.M. Dzhagarov [b], E.P. Petrov [c], P.T. Petrov [a,*]

[a] Scientific Pharmaceutical Center, RUE Belmedpreparaty, Fabritsius Street 30, 220007 Minsk, Belarus
[b] B.I. Stepanov Institute of Physics, National Academy of Sciences of Belarus, Nezavisimosti Avenue 68, 220072 Minsk, Belarus
[c] Biophysics, BIOTEC, Technische Universität Dresden, Tatzberg 47-51, 01307 Dresden, Germany

ARTICLE INFO

Article history:
Received 6 December 2007
Received in revised form 30 May 2008
Accepted 17 June 2008
Available online 24 June 2008

Keywords:
Chlorin e6
Polyvinylpyrrolidone
Photodynamic therapy
Photolon
Fotolon
Complexation

ABSTRACT

It is recognized that chlorin e6–polyvinylpyrrolidone (Ce6–PVP) formulations are characterized by a high efficacy in photodynamic therapy of malignant tumors. Currently, a commercially available formulation of this type is Photolon® (Fotolon®) with Ce6:PVP = 1:1 (w/w) and the weight-average molecular weight of PVP is 1.2×10^4. To gain a better understanding of the role played by PVP in Ce6–PVP formulations, we carry out experiments on IR and UV–VIS absorption, steady-state and time-resolved fluorescence, time-resolved triplet–triplet absorption, octanol–water partitioning, and solubility of chlorin e6 in buffer solutions at pH 6.3, 7.4, and 8.5 in presence of PVP with Ce6:PVP ratios ranging from 1:0 to 1:1000 (w/w) for PVP samples with weight-average molecular weights of 8×10^3, 1.2×10^4, and 4.2×10^4. We show that Ce6 interacts with PVP by forming molecular complexes via hydrophobic interactions and determine the Ce6–PVP binding constant, as well as the mean number of PVP monomers per binding site. We find that complexation of Ce6 with PVP prevents Ce6 aggregation in aqueous media and leads to an enhancement of Ce6 fluorescence quantum yield, while keeping the quantum yield of the intersystem crossing essentially unchanged. Possible scenarios of how the presence of PVP can favorably affect the PDT efficacy of chlorin e6 in Ce6–PVP formulations are discussed.

© 2008 Elsevier B.V. All rights reserved.

1. Introduction

The availability of efficient biocompatible photosensitizers is imperative for successful development and clinical applications of the photodynamic therapy (PDT) [1]. Therefore, research and development of new effective photosensitizing agents is an important objective determining the further progress in the field of the cancer therapy. An improvement of photophysical and pharmacokinetic parameters of new photosensitizers can be achieved by either chemical or non-covalent modifications of photosensitizing molecules with polymers [1–4]. Photosensitizer modifications were obtained by their incorporation into polymer microspheres [5], binding to insulin molecules [6], or conjugation to polyethylene glycol [7] or tumor tissue-specific monoclonal antibodies [8]. In a number of cases stable complexes based only on intermolecular interactions of a photosensitizer with a polymer could also be obtained [4]. In particular, polyvinylpyrrolidone (PVP), being a water soluble and non-toxic polymer [9], is widely used to modify water solubility, pharmacokinetics and pharmacological (including antitumor) activity of various biologically active compounds [10–12]. Indeed, the presence of PVP was shown to accelerate photosensitized oxidation of chlorophyll derivatives *in vitro* [13] and increase the antitumor activity of tumor necrosis factor-alpha [14].

Chlorin e6 (Ce6) is a promising photosensitizer characterized by a high sensitizing efficacy and rapid elimination from the body [15]. Photosensitizer Photolon® (also known as Fotolon®), a formulation containing a complex of Ce6 and PVP ($\bar{M}_w = 1.2 \times 10^4$) at the ratio of 1:1 (w/w) [16,17], originally developed at the Scientific Pharmaceutical Center of RUE Belmedpreparaty (Minsk, Belarus), has been proven to be effective in photodynamic diagnostics and treatment of different cancerous and non-oncological diseases [18–20]. Since 2002, Photolon® (Fotolon®) is registered in the Republic of Belarus and Russian Federation and approved for medical application as a means for photodynamic diagnostics and therapy of malignant tumors of skin and mucous membranes. Comparative assessment of the pharmacokinetic properties and PDT activity of Ce6 and the Ce6–PVP formulation revealed that Ce6–PVP more selectively accumulates and longer retains in the tumor tissue, and, at the same time has a faster clearance rate

* Corresponding author.
E-mail address: petr_petrov@tut.by (P.T. Petrov).
[1] These authors contributed equally to this work.

1011-1344/$ - see front matter © 2008 Elsevier B.V. All rights reserved.
doi:10.1016/j.jphotobiol.2008.06.004

from skin and normal tissues than Ce6 alone [16,19–21]. In our *in vivo* studies we have observed that the photosensitizing activity and the subsequent tumor necrosis are substantially higher for Ce6–PVP at Ce6:PVP = 1:1 w/w than for Ce6 alone [22] and that a further improvement of the PDT efficacy is observed when the PVP content in the formulation is increased [23]. However, the molecular mechanisms of the enhanced photodynamic activity of the Ce6–PVP composition are still not clearly understood. In particular, the following questions need to be answered: What is the role of the polymer in providing the high PDT efficacy of the formulation? Is the enhanced photodynamic activity of Ce6–PVP related to the improved photophysical properties of the photosensitizer–polymer complex, or, rather, the presence of the polymer prevents premature chemical modification and aggregation of Ce6?

In our previous study [24], we have found that Ce6 can form molecular complexes with PVP in solution, and that the interaction of Ce6 with the polymer leads to pronounced changes in photophysical parameters of Ce6. However, quantitative description of the interaction between Ce6 and PVP, evaluation of the Ce6–PVP complex stability, as well as assessment of the modification of the physico-chemical properties of Ce6 upon complexation with PVP remained to be investigated. In addition, the well known fact of pH differences between the normal and cancerous tissue [25] along with the strong effect of pH on the photophysical properties of Ce6 [26] poses the question whether the pH effect on Ce6 photophysics is affected by complexation with PVP.

Giving answers to the above question will provide better grounds for understanding the high photodynamic efficacy of Photolon® (Fotolon®) and related Ce6–PVP formulations compared to Ce6 alone.

2. Materials and methods[2]

2.1. Chlorin e6 and its esters

Chlorin e6 (Fig. 1) (96.5% purity by HPLC) was synthesized by a modified method of Lötjönen and Hynninen [27] at RUE Belmedpreparaty (Minsk, Belarus). Chlorin e6 17^4-ethyl ester (98.1%), referred to in what follows as Ce6 monoethyl ester, and chlorin e6 17^4, 15^3-diethyl ester (99.0%), referred to in what follows as Ce6 diethyl ester, were synthesized by partial esterification of Ce6 in 4% H_2SO_4/ethanol medium, followed by fractionation of the ester mixture by preparative reversed-phase HPLC. Purity of compounds was determined by normalization using an HPLC-based method described elsewhere [28,29]. Dark glassware and freshly prepared solutions were used to avoid unwanted Ce6 photodegradation. Sample handling and all measurements were carried out at room temperature (25 ± 1 °C).

2.2. Polyvinylpyrrolidones

Three different samples of polyvinylpyrrolidone (Fig. 1) were used in the present work: PVP K15 and PVP K30 (Aldrich, USA), and PVP with the quoted weight-average molecular weight of $(1.26 \pm 0.27) \times 10^4$ (AK Sintvita, Russia) referred to in what follows as PVP K19. The exact weight-average molecular weights $\bar{M}_w$ and polydispersities $\bar{M}_w/\bar{M}_n$, where $\bar{M}_n$ is the number-average molecular weight, of these PVP samples were determined by size-exclusion chromatography and are presented in Table 1.

[2] All experiments carried out in the present study were repeated in at least three independent attempts, and good agreement between results of measuments was found.

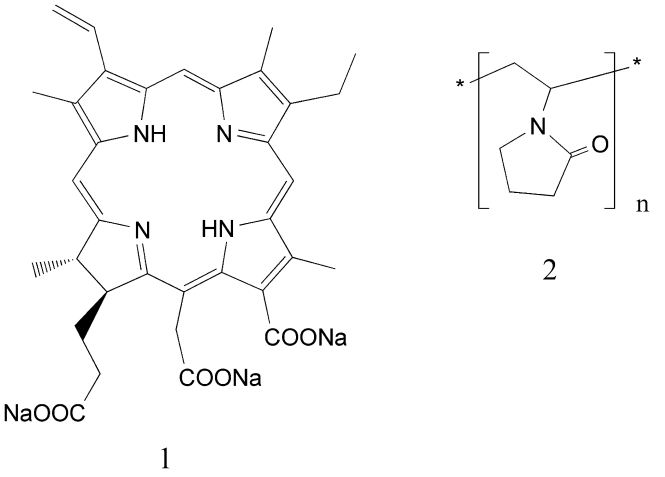

Fig. 1. Chemical structures of chlorin e6 trisodium salt (1) and polyvinylpyrrolidone (2).

Table 1
Molecular weight characteristics of PVP samples, as determined by SEC-HPLC

Sample	$\bar{M}_w$	$\bar{M}_w/\bar{M}_n$	$\bar{M}_w$ of 5% high-molecular fraction
PVP K15	8200	3.8	27,500
PVP K19	11,700	4.1	40,500
PVP K30	41,800	4.3	152,000

2.3. Preparation of solutions of Ce6 and Ce6–PVP complex

Ce6 was preliminarily dissolved in a droplet of 0.1% NaOH, and PVP was predissolved in appropriate buffers (phosphate buffer solutions (0.01 M) of pH 6.3, 7.4, 8.0, and 8.5). Stock solutions were subsequently prepared to yield Ce6:PVP weight ratio (w/w) from 1:0 to 1:1000 and afterwards diluted with appropriate buffers. pH values of the final solutions of Ce6 and Ce6–PVP were measured using an HI 8314 pH-meter (Hanna Instruments) before the experiments and adjusted if necessary.

2.4. Size-exclusion chromatography of PVP

The size-exclusion chromatography (SEC-HPLC) analysis of the molecular weight parameters of PVP was carried out on a chromatography system consisting of a Waters 600E pump and Waters 410 refractive index detector (Waters Corp., Milford, USA). Separation was performed using a mobile phase consisting of 0.1 M $NaNO_3$ solution on a Shodex KB-803 column (Showa Denko, Japan). The column was calibrated with pullulan $\bar{M}_w$ standards (Showa Denko, Tokyo, Japan).

2.5. Solubility investigation

Solubility of Ce6, its monoethyl and diethyl esters, and their complexes with PVP K19 (concentration of Ce6 2 mg/ml) in a buffer solution (0.1 M, pH 8.0) was evaluated by measuring the concentration of the Ce6 in solution after centrifugation (10,000 rpm, 10 min). The quantity of the dissolved substance was calculated by measuring the differences in absorbance at 663 nm of freshly prepared and centrifuged solutions. This wavelength was chosen from the practical point of view to facilitate absorption measurements at relatively high concentrations of Ce6; additionally, the use of the long wavelength strongly reduces the potential contribution of light scattering on molecular aggregates at high concentrations and thus helps to avoid possible experimental artifacts.

2.6. Octanol–water partition coefficients

Lipophilic and hydrophilic properties of Ce6 and Ce6–PVP formulations were characterized by the partition coefficient $D_{o/w} = C_o/C_w$ of the compound between the two immiscible solvents *n*-octanol (o) and 0.1 M phosphate buffer, pH 7.4 (w). Measurements were carried out as described by Bourre et al. [30]. The measurements were carried out using PVP K19.

2.7. Steady-state fluorescence and absorption measurements

Absorption spectra were recorded on a Shimadzu UV2401PC spectrophotometer (Shimadzu Corp., Japan) in quartz cuvettes. Fluorescence spectra corrected for the spectral response of the detection system and polarized fluorescence spectra were recorded on a spectrofluorimeter described elsewhere [31]. The fluorescence quantum yield φ was determined by the relative method using a solution of Ce6 in the buffer at pH 8.5 with the reported quantum yield of 0.18 [24] as a fluorescent standard. Fluorescence spectra and the fluorescence quantum yield were measured using the excitation wavelength of 407 nm. The relative accuracy of fluorescence quantum yield determination was 5%. The degree of fluorescence polarization P was measured with the excitation at 650 nm. The absolute accuracy of the fluorescence polarization degree was 0.07. Concentration of Ce6 in samples did not exceed 2.0×10^{-5} M for absorption measurements (particular values are given in figure legends) and 5.0×10^{-6} M for steady-state fluorescence measurements. Low excitation power densities were used in steady-state fluorescence and absorption measurements to avoid photodegradation of Ce6 samples.

2.8. Time-resolved fluorescence and triplet–triplet absorption measurements

The lifetimes of the excited singlet state τ_S of Ce6 were determined by measuring fluorescence decays using a modified PRA-3000 pulse fluorometer (Photochemical Research Associates, London, Ontario) operating in the time-correlated single photon counting mode [32]. The concentration of Ce6 was 5.0×10^{-6} M. Measurements were carried out at a low excitation power density, and no signs of sample photodegradation during time-resolved fluorescence measurements were detected. The lifetimes of the excited singlet state were determined by the non-linear least-squares reconvolution analysis of fluorescence decay curves [32] assuming a single-exponential fluorescence decay law $F(t) = F(0)\exp(-t/\tau_S)$. The estimated relative errors in fluorescence lifetimes were about 3%.

Kinetics of the triplet–triplet absorption [33] were measured on a home-made laser flash photolysis spectrometer. In particular, samples were excited by the second harmonic of a Nd^{3+}:YAG laser (excitation wavelength 532 nm, pulse duration 15 ns). The triplet–triplet absorption was probed using a DKsSh-120 xenon lamp. A MS 2004i monochromator (SOLAR TII, Minsk, Belarus) was used to select the detection wavelength, which was set to 450 nm in our experiments. The optical signal was detected by a FEU-128 photomultiplier tube with a time resolution of 20 ns. The concentration of Ce6 was 2.0×10^{-5} M. The relative errors of the measured amplitudes of triplet–triplet absorption did not exceed 7%. In contrast to steady-state absorption and fluorescence measurements, and time-resolved fluorescence experiments, measurements of the triplet–triplet absorption kinetics require much higher excitation power densities. Therefore, to ensure reliable results, the extent of photodegradation of samples during triplet–triplet absorption experiments was carefully monitored. In cases where absorbance of a sample changed by more than 3% at the $Q_x(0,0)$ absorption maximum during the measurement, the results were discarded, and the sample was replaced by a freshly prepared one. The triplet state lifetimes τ_T were determined by the non-linear least-squares fitting of triplet–triplet absorption decay curves to a single-exponential $\Delta A(t) = \Delta A(0)\exp(-t/\tau_T)$ or double-exponential $\Delta A(t) = \Delta A(0)(a_1\exp(-t/\tau_{T1}) + a_2\exp(-t/\tau_{T2}))$ decay law. The estimated relative error in the triplet state lifetime determination was about 10%.

2.9. Infrared spectroscopy measurements

Infrared absorption spectra were recorded on a Nicolet 5DXB FT-IR spectrophotometer in the spectral range of 4000–400 cm^{-1} at an effective resolution of 2 cm^{-1}. Solid dispersions of the different systems were obtained by lyophilization of Ce6–PVP aqueous solutions (at Ce6:PVP ratios 1:0.1, 1:1, and 1:10 (w/w)). Residual solvent was removed by drying under vacuum at the room temperature for 2 days, after which the samples were mixed with dry KBr to form pellets.

3. Results and discussion

3.1. Photophysical properties of Ce6–PVP at pH 8.5

UV–VIS absorption and fluorescence spectra of Ce6 in solution at pH 8.5 (Figs. 2 and 3) show a pronounced dependence on the amount of PVP (a qualitatively similar picture is observed at other pH values – see below), thus giving the evidence of intermolecular photosensitizer–polymer interactions. In particular, the absorption spectra show isosbestic points at 407, 546, 556, 606, 618 and 658 nm. In a similar manner, the fluorescence spectra of Ce6 solutions at varying concentrations of PVP show, when excited at an isosbestic point, several isostilbic points. They are, however, not observed in Fig. 3 due to the amplitude normalization of the fluorescence spectra. A similar behavior of the absorption and fluorescence spectra has been reported previously for Ce6 upon its binding to liposomes and human serum albumin [34–36]. We note that, starting with Ce6:PVP ≈ 1:500 w/w, the further increase in

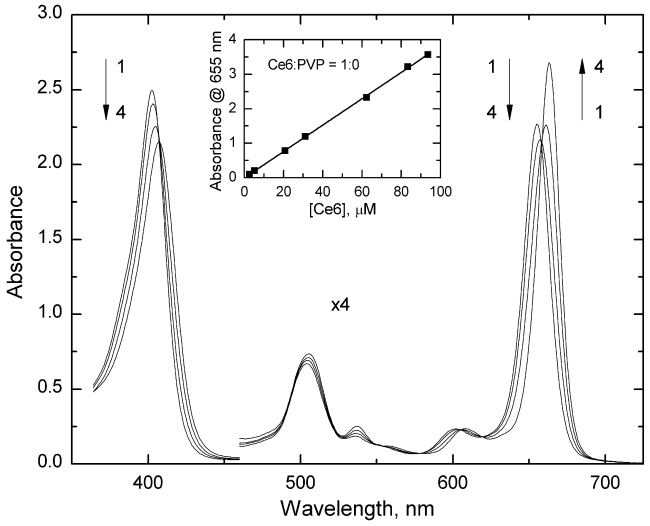

Fig. 2. Absorption spectra of Ce6 at different concentrations of PVP K19 in buffer solution (pH 8.5). Ce6:PVP w/w ratios: 1:0 (1), 1:9 (2), 1:36 (3), and 1:1000 (4). [Ce6] = 1.44×10^{-5} M; 1-cm cuvette. Inset shows the concentration dependence of the absorbance of Ce6 at 655 nm in the absence of PVP in a buffer solution (pH 8.5) as a function of the Ce6 concentration. The linear fit $A(\lambda = 655\ nm) = a[Ce6] + b$, where $a = 0.0382 \pm 0.0003$, $b = -0.006 \pm 0.019$, and [Ce6] is given in μM, indicates that no Ce6 aggregation takes place under these conditions within the specified concentration range.

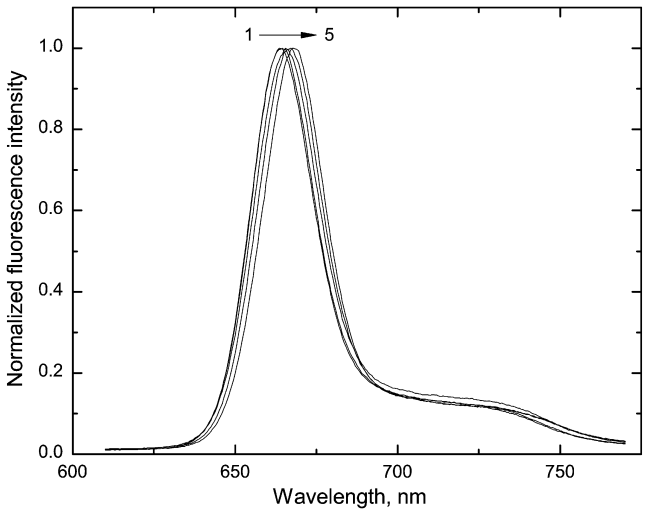

Fig. 3. Normalized fluorescence spectra of Ce6 ([Ce6] = 5.0×10^{-6} M) at different concentrations of PVP K19 in buffer solution (pH 8.5). Ce6:PVP w/w ratios: 1:0 (1), 1:10 (2), 1:30 (3), 1:70 (4), and 1:1000 (5). Excitation wavelength 407 nm.

the PVP content does not lead to any noticeable changes in the absorption and fluorescence spectra of Ce6.

It is known, that upon a concentration increase, Ce6 molecules tend to aggregate in solution (see, e.g. [26,38]). Since uncontrolled presence of Ce6 aggregates may significantly affect the conclusions drawn from our experiments, we determined the range of Ce6 concentrations within which aggregate formation can be neglected in a Ce6 solution at pH 8.5 in the absence of PVP. Measurements of the absorption spectrum for a set of seven samples covering the range of Ce6 concentrations of $(2.6\ldots94) \times 10^{-6}$ M have shown that no noticeable changes in the shape of the absorption spectrum of Ce6 take place, and the ratio of absorbances at the maxima of the Soret band and the Q-bands stays constant within the whole concentration range. The linear dependence of Ce6 absorbance with a zero intercept (see inset in Fig. 2) for $[Ce6] = (2.6\ldots94) \times 10^{-6}$ M clearly shows that no aggregates are formed for Ce6 concentrations up to ca. 90 μM. Therefore, in all our experiments, we chose to use Ce6 concentrations not exceeding 2.0×10^{-5} M.

Photophysical properties of Ce6 solutions without PVP and at the Ce6:PVP ratio of 1:1000 w/w are summarized in Table 2. The absorption spectrum of Ce6 in the buffer solution at pH 8.5 in the absence of PVP is characterized by a strong Soret band with the maximum at 402 nm and weaker Q-bands in the region of 450–700 nm. In agreement with our previous results [24], we have found that an increase in the PVP content in solution (pH 8.5) at a constant Ce6 concentration produces a red shift of absorption (Fig. 2) and fluorescence (Fig. 3) bands and additionally leads to an increase in the fluorescence quantum yield (by a factor of ~1.3), fluorescence lifetime (by a factor of ~1.2) and fluorescence polarization degree of Ce6. Moreover, the measured degree of Ce6 fluorescence polarization of 0.20 at Ce6:PVP = 1:1000 indicates that the rotational diffusion of Ce6 is substantially inhibited in the presence of PVP, which allowed us to conclude on formation of molecular complexes of Ce6 with bulky PVP molecules.

Using time-resolved triplet–triplet absorption studies we have found that in the absence of PVP, the transient triplet–triplet absorption decays according to the monoexponential law $\Delta A(t) = \exp(-t/\tau_T)$ with the lifetime $\tau_T \approx 2$ μs. However, when the PVP content was a factor of 15 or higher than that of Ce6 (w/w), the decay of the transient triplet–triplet absorption was better described by the biexponential law with $\tau_{T1} \approx 2$ μs and $\tau_{T2} \approx 5.2$ μs (Fig. 4). Moreover, the relative contribution of the longer-lived component gradually increased with the PVP content (Table 3). These observations allowed us to attribute the longer-lived component of the triplet–triplet absorption to Ce6 molecules bound to the polymer. This conclusion was further confirmed by comparison of these results with the data on Ce6 binding to PVP (see below).

The triplet state lifetime τ_T of chlorophyll-related compounds is known to be strongly dependent on the oxygen concentration: $1/\tau_T = 1/\tau_{T0} + k_q[O_2]$, where τ_{T0} is the triplet state lifetime in the oxygen-free solution, and k_q is the effective rate constant the triplet state quenching by oxygen (for more details on the triplet state quenching by oxygen in chlorophyll-related compounds, see, e.g. [37]). Our preliminary experiments have shown that the triplet lifetimes τ_{T0} of Ce6 and Ce6–PVP (Ce6:PVP = 1000) in oxygen-free buffer solutions are ~200 and ~500 μs, respectively, in agreement with previously reported values [38,39]. Therefore, the increase in the triplet state lifetime of Ce6 upon its complexation with PVP should be attributed to a reduction in the effective oxygen quenching constant due to a reduced accessibility of Ce6 to oxygen molecules as a result of steric hindrances introduced by the polymer matrix.

At the same time, the amplitude of the triplet–triplet absorption of Ce6 is virtually unaffected by the presence of the polymer (Table 2). This, taken along with the observed increase in the fluorescence quantum yield upon complexation with PVP (from 0.18 to 0.24), allowed us to conclude that the quantum yield of the intersystem crossing of Ce6 did not decrease by more than ~10% upon its complexation with PVP. Taking into account that the quantum yield of singlet oxygen production is closely correlated with the quantum yield of the intersystem crossing [37], we conclude that the quantum yield of singlet oxygen generation by Ce6 does not change by more than ~10% upon its complexation with PVP (the latter conclusion, of course, needs to be verified in independent direct experiments).

Thus, the Ce6–PVP complex, as compared to free Ce6, is characterized by a higher fluorescence quantum yield, more intense and

Table 2
Photophysical properties of Ce6 and Ce6–PVP K19 (Ce6:PVP = 1:1000 w/w) in solution at pH 8.5, 7.4, and 6.3

pH	Sample	λ_{max}^{Soret} (nm)	$\lambda_{max}^{Q(0,0)}$ (nm)	$\Delta\bar{\nu}_{abs}$ (cm^{-1})	λ_{max}^{f} (nm)	φ	τ_S (ns)	P	$\Delta A^*/\Delta A_0^*$	τ_T (μs)[a]
8.5	Ce6	402	654	490	662	0.18	4.4	0.00	1.00	1.8
	Ce6–PVP	405	663	430	670	0.24	5.1	0.20	1.02	5.3
7.4	Ce6	402	654	490	662	0.18	4.3	0.00	0.98	2.1
	Ce6–PVP	405	663	430	670	0.24	5.1	0.18	0.96	5.7
6.3	Ce6	405	645	690	659	0.16	3.8	0.01	0.82	2.0
	Ce6–PVP	405	663	450	669	0.25	5.2	0.22	1.00	5.0

Note. λ_{max}^{Soret} и $\lambda_{max}^{Q(0,0)}$ are the maxima of the Soret and $Q_x(0,0)$ absorption bands, respectively; $\Delta\bar{\nu}_{abs}$ is the full width at half maximum of the $Q_x(0,0)$ absorption band; λ_{max}^{f} is the maximum of the fluorescence band; φ is the fluorescence quantum yield; P is the degree of fluorescence polarization; $\Delta A^* = \Delta A_{TT}/A(\lambda_{exc})$ is the reduced amplitude of the triplet–triplet absorption, where ΔA_{TT} is the experimentally observed amplitude of triplet–triplet absorption, and $A(\lambda_{exc})$ is the absorbance of the sample at the excitation wavelength; ΔA_0^* is the reduced amplitude of the triplet–triplet absorption of Ce6 at pH 8.5; τ_S is the lifetime of the first excited singlet state of Ce6; τ_T is the lifetime of the first excited triplet state of Ce6.

[a] For Ce6–PVP, τ_T was measured at Ce6:PVP = 1:500 w/w.

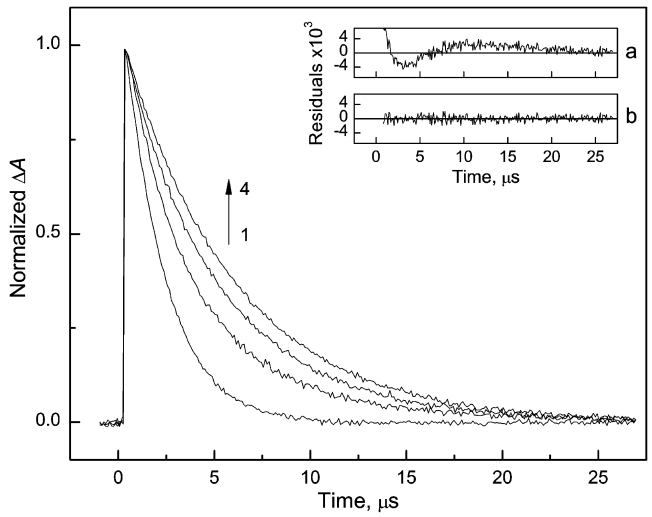

Fig. 4. Normalized kinetics of triplet–triplet absorption of chlorin e6 ([Ce6] = 2.0×10^{-5} M) at different concentrations of PVP K19 in buffer solution (pH 8.5). Ce6:PVP w/w ratios: 1:0 (1), 1:15 (2), 1:50 (3), and 1:100 (4). Inset shows residuals for the single- (a) and double-exponential (b) fits of curve (2). Excitation wavelength 532 nm; detection wavelength 450 nm.

Table 3
Triplet state lifetimes and their relative contributions to the triplet–triplet absorption kinetics for Ce6 and Ce6–PVP K19 with different Ce6:PVP weight ratios at pH 8.5

Ce6:PVP ratio (w/w)	Fast component		Slow component	
	τ_{T1} (μs)	a_1	τ_{T2} (μs)	a_2
1:0	1.8 ± 0.2	1.00	–	–
1:1	2.0 ± 0.2	1.00	–	–
1:15	2.0 ± 0.2	0.58 ± 0.06	5.2 ± 0.4	0.42 ± 0.04
1:50	1.9 ± 0.2	0.27 ± 0.03	5.2 ± 0.4	0.73 ± 0.07
1:100	2.2 ± 0.2	0.18 ± 0.02	5.6 ± 0.5	0.82 ± 0.08
1:500	–	–	5.3 ± 0.4	1.00

red shifted absorption band, and just a slightly decreased quantum yield of intersystem crossing. Therefore, a certain improvement in PDT-related photophysical properties of Ce6 is indeed observed upon its binding to PVP. However, in our opinion, the extent of this modification observed for PVP-bound Ce6 can hardly explain the substantial increase in PDT efficiency consistently observed in *in vivo* PDT experiments and medical applications of the Ce6–PVP complex (Photolon®, Fotolon®) in comparison with free Ce6 [22] (for discussion, see below).

3.2. Effect of pH on properties of Ce6–PVP complex

It is known that tumor tissues can have pH values differing from those of the normal tissue [25]. However, in the absence of exact data on pH values of particular tumors successfully treated with Photolon® (Fotolon®), a study of properties of the Ce6–PVP complex within a wide range of pH values would help to estimate and understand effects which can in principle be observed in tumor tissues.

First, we addressed the photophysical properties of free Ce6 and Ce6–PVP complex with Ce6:PVP = 1:1000 in buffer solutions at physiologically important pH values 7.4 and 6.3. The summary of our results is presented in Table 2.

In particular, we found that in the absence of polymer, there are no significant differences in the photophysical properties of Ce6 in solution at pH 7.4 and pH 8.5. However, at pH 6.3 a red shift and broadening of Soret band, as well as a blue shift and broadening of $Q_x(0,0)$ absorption and fluorescence bands of Ce6 were observed. These observations are in a good agreement with the results of Čunderlíková et al. [26]. Additionally, at pH 6.3 we observed a slight decrease in the fluorescence quantum yield from 0.18 to 0.16 and shortening of the fluorescence lifetime from 4.4 to 3.8 ns for free Ce6. At the same time, time-resolved triplet–triplet absorption experiments showed that at pH 6.3 the amplitude of Ce6 triplet–triplet absorption decreased by ~18% as compared with the one at pH 8.5, whereas the lifetime of triplet state of Ce6 molecules remained virtually unchanged (2.0 μs). These changes in the Ce6 photophysics can be caused by neutralization of carboxyl groups leading to an increased hydrophobicity and therefore aggregation of Ce6 molecules at lower pH.

Addition of PVP to Ce6 solutions (Ce6:PVP = 1:1000) at pH 7.4 and pH 6.3 resulted in changes of photophysical properties of Ce6 similar to those observed at pH 8.5 (see Table 2). The most drastic changes including a substantial red shift of the $Q_x(0,0)$ absorption (by ~18 nm) and fluorescence (by ~10 nm) bands, an increase in the fluorescence quantum yield (by a factor of ~1.7), degree of polarization (from 0 to 0.22), triplet–triplet absorption (by a factor of ~1.2), singlet (by a factor of ~1.4) and triplet (by a factor of ~2.5) lifetimes, have been detected for Ce6 at pH 6.3 (see Table 2 and Figs. 5 and 6).

Notice that at Ce6:PVP weight ratio of 1:1000, when, as is shown below, essentially all photosensitizer molecules are bound to the polymer, the photophysical properties of Ce6 are virtually independent of the solution pH. Therefore, within the pH range studied, the microenvironment of the PVP-bound photosensitizer is not affected by pH, which means that Ce6 molecules are incorporated into the polymer matrix in a pH-independent way. The maximum and full width at half maximum of the $Q_x(0,0)$ absorption and fluorescence bands, fluorescence quantum yield, and singlet state lifetime of Ce6–PVP at Ce6:PVP = 1:1000 w/w closely correlate with the corresponding parameters of Ce6 in organic solvents with the dielectric constant ranging from 20 to 35 [24,31,34]. These findings allow us to conclude that PVP-bound Ce6 molecules are localized in hydrophobic domains of the polymer, similar to what was concluded for Ce6 bound to proteins and liposomes [34–36,40].

Additionally, it is known that Ce6 molecules in polar organic solvents, alkaline aqueous media, and when bound to proteins, liposomes and cells stay predominantly in the monomeric form

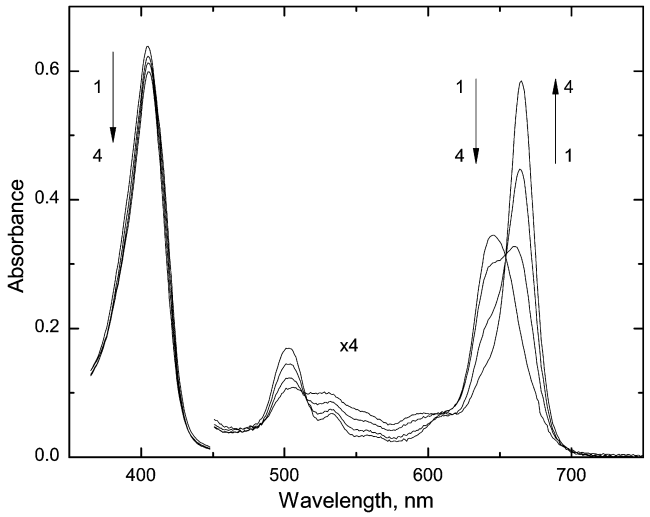

Fig. 5. Absorption spectra of Ce6 at different concentrations of PVP K19 in buffer solution (pH 6.3). Ce6:PVP w/w ratios: 1:0 (1), 1:15 (2), 1:50 (3), and 1:100 (4). [Ce6] = 2.0×10^{-5} M; 0.2-cm cuvette.

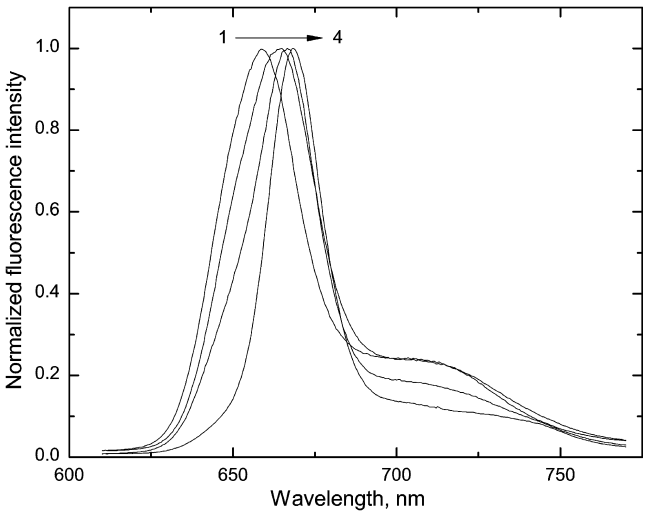

Fig. 6. Normalized fluorescence spectra of Ce6 ([Ce6] = 5.0×10^{-6} M) at different concentrations of PVP K19 in buffer solution (pH 6.3). Ce6:PVP w/w ratios: 1:0 (1), 1:15 (2), 1:50 (3), and 1:100 (4). Excitation wavelength 407 nm.

[26,35,38,41]. Therefore, we may speculate that, in a similar manner, complexation with PVP prevents Ce6 aggregation or even disrupts pre-existing Ce6 aggregates, thus preserving the monomeric form of the photosensitizer.

To verify this assumption, we studied the effect of the presence of PVP on aggregation of Ce6 in aqueous solution of low ionic strength. In particular, we have found that the absorption spectrum of a solution of Ce6 in distilled water kept in a dark place at the room temperature gradually transforms with time, revealing a decrease and broadening of the Soret and $Q_x(0,0)$ absorption bands within 90 min (Fig. 7). Since Ce6 is a weak acid, these spectral changes are obviously associated with the hydrolysis of the Ce6 salt and subsequent aggregation of partially protonated molecules. In contrast, in the presence of PVP in solution, no visible changes were observed in absorption spectrum of the solution even after 5 h. Thus, we conclude that complexation of Ce6 with PVP indeed prevents hydrolysis and subsequent aggregation of the photosensitizer, which is known to be beneficial for the PDT efficacy [4].

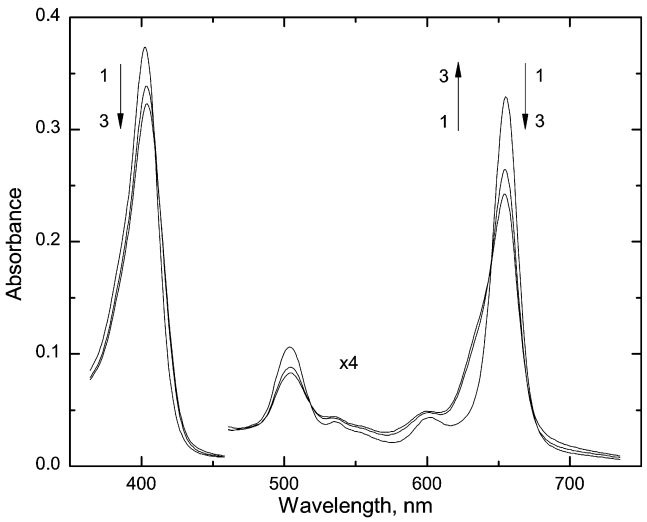

Fig. 7. Temporal changes in absorption spectra of Ce6 sodium salt in distilled water: immediately after dissolution (1), after 30 min (2), and after 90 min (3). [Ce6] = 2.0×10^{-6} M; 1-cm cuvette.

3.3. Mechanism of PVP interaction with Ce6 and its esters

The pronounced propensity of PVP to interact with Ce6 in solutions at a range of pH values and ionic strengths prompted us to make a more detailed investigation of the mechanisms of Ce6–PVP complexation. It is recognized that PVP can act as a proton acceptor (through either the O or N atoms of the pyrrole ring) hydrogen bonds can be formed between PVP and the drug [9]. As regards Ce6, it can donate hydrogens from the NH groups of the macrocycle or the three COOH residues. However, it is clear that the aromaticity of the chlorin cycle strongly prevents imine's hydrogens from H-bonding. The strength of hydrogen bonds formed via carboxylic groups has to be substantially influenced by pH of the solution, becoming much weaker in alkaline media (at pH > 8) where Ce6 carboxyls are ionized. However, as we have observed earlier, the photophysical properties of the Ce6–PVP complex are almost the same at slightly acidic and alkaline solutions. For this reason, it was our intention to examine if Ce6 carboxyl moieties really act as the principal bonding means with the PVP. The investigation of this effect was carried out by comparing FT-IR spectra of lyophilized Ce6–PVP complex with those of a mechanical mixture of these two compounds. There is a number of works showing that positions of vibrational bands of the groups involved in the H-bonding (such as carbonyls of PVP and carboxyls of the Ce6 in the present case) undergo noticeable changes compared to a simple linear superposition of the spectra of the individual compounds (see, e.g. [42]).

However, in our experiments, the FT-IR spectra of physical mixtures of Ce6 and PVP and lyophilized Ce6–PVP complexes at Ce6:PVP ratios of 1:0.1, 1:1 and 1:10 (w/w) appeared to be identical within the experimental error (data no shown), and the spectra of the lyophilized Ce6–PVP can be simply regarded as the superposition of the spectra of the Ce6 and PVP. Thus, based on the fact that no changes were detected in the characteristic bands (O–H, C=O) the dominating role of hydrogen bonding in Ce6–PVP interaction can be clearly ruled out.

To further check this conclusion, we studied esterified Ce6 derivatives having fewer carboxyl groups and therefore dramatically less soluble than Ce6 even under alkaline conditions. The effect of PVP on solubilization of Ce6, mono- and diethyl esters of Ce6 was investigated at the concentration close to that used in clinical practice (2 mg/ml). At this concentration, Ce6 is completely soluble in aqueous media, whereas, according to our measurements, only 95% and 12% of more hydrophobic mono- and diethyl esters of Ce6 remained in solution, respectively. However, in the presence of PVP, at the Ce6 derivative:PVP ratio of 1:10, the amount of the dissolved substances increased to 100% and 60%, respectively. Thus, the solubilizing effect of PVP is sufficient to maintain substances more hydrophobic than Ce6 in solution at relatively high concentrations. Similar observations have been reported previously for another photosensitizer formulation containing a hydrophobic photosensitizer hypericin and PVP [43]. Presumably, in the case of the less polar Ce6 derivatives, weak non-specific interactions (via, e.g., ion–dipole and dispersion forces) with PVP are responsible for this solubilizing effect of PVP.

3.4. Ce6–PVP binding constant

A step toward answering the still unresolved question whether Ce6, upon introduction of Ce6–PVP *in vivo*, stays bound to PVP, as well as the related question on the molecular mechanisms of the Ce6 (or Ce6–PVP) transport via the cell membrane, can be made by studying the parameters of Ce6–PVP binding. In particular, we are interested in the Ce6–PVP binding constant and the number of PVP monomers per binding site. Additionally, in view of the inherent polydispersity of PVP used as a carrier in medicinal

applications (see Table 1), it is of interest to verify whether these binding parameters are dependent on the polymerization degree of PVP.

As it was mentioned above, Ce6 molecules tend to aggregate in aqueous media, especially under acidic conditions [26]. Thus, to avoid ambiguity which can be introduced by aggregation, Ce6 binding to PVP was studied under the conditions where chlorin molecules are monomeric: i.e. in an alkaline medium (pH 8.5) at Ce6 concentrations not exceeding 2×10^{-5} M (see inset in Fig. 2).

The minimal model capable of providing a quantitative answer to this question assumes that each PVP polymer molecule can provide several independent sites for Ce6 binding. In this case, the following relation holds [44]:

$$[L_{\text{bound}}]/[M] = K[L_{\text{free}}]/\{n(1 + K[L_{\text{free}}])\} \quad (1)$$

where $[L_{\text{bound}}]$ and $[L_{\text{free}}]$ are the concentrations of the bound and free ligand (Ce6), $[M]$ is the concentration of PVP macromolecules expressed here as a molar concentration of PVP monomers in solution, n is the number of PVP monomers per binding site, and K is the association (binding) constant of the Ce6–PVP complex. The fraction of the bound photosensitizer $x = [L_{\text{bound}}]/[L_0]$, where $[L_0] = [L_{\text{free}}] + [L_{\text{bound}}]$ is the total concentration of Ce6, is expressed as follows:

$$x = \Big(1/K + [M]/n + [L_0] - \sqrt{(1/K + [M]/n + [L_0])^2 - 4[L_0][M]/n}\Big) \Big/ (2[L_0]) \quad (2)$$

The fraction x of PVP-bound Ce6 was determined from a set of absorption spectra at a fixed total Ce6 concentration of 1.44×10^{-5} M with the Ce6:PVP ratio varying from 1:2 to 1:200 w/w by assuming that the Ce6 absorption spectrum $A(\lambda)$ at a given PVP concentration is a linear superposition of the spectra of bound and free Ce6 molecules $A_{\text{bound}}(\lambda)$ and $A_{\text{free}}(\lambda)$, respectively:

$$A(\lambda) = xA_{\text{bound}}(\lambda) + (1 - x)A_{\text{free}}(\lambda), \quad 0 < x < 1 \quad (3)$$

Unfortunately, the spectrum of PVP-bound Ce6 $A_{\text{bound}}(\lambda)$ is not available directly. To obtain its experimental estimate, we made use of the observation that the effect of the polymer on the photophysical properties of Ce6 saturates at high polymer concentrations and becomes independent of the polymer content starting with Ce6:PVP ≈ 1:500, which can be interpreted as an indicative of virtually all Ce6 molecules being bound to PVP. Therefore, the absorption spectrum of Ce6–PVP at Ce6:PVP = 1:1000 was taken as a reasonable experimental estimate of $A_{\text{bound}}(\lambda)$.

We have found out that representation Eq. (3) provided an excellent description of the Ce6 absorption spectra in the presence of PVP within the whole range of Ce6:PVP ratios from 1:2 to 1:200 (w/w) for all three PVP samples used in the present study. The estimated values of the fraction x of the PVP-bound Ce6 are presented for PVP K19 in Fig. 8 as a function of the PVP monomer concentration. Qualitatively similar dependences were obtained for PVP K15 and PVP K30.

It is remarkable that the relative contribution of the longer-lived component of the triplet state decay of Ce6 (Table 3) closely follows the behavior of the bound fraction of Ce6 (Fig. 8), which serves as an additional confirmation of its assignment to PVP-bound Ce6 molecules (see Section 3.1).

The binding parameters K and n were determined from the dependences of the PVP-bound fraction x of Ce6 on the PVP monomer concentration by non-linear least-squares fitting with Eq. (2). For all three polymers, Eq. (2) provided excellent fits to the dependences, which is exemplified in Fig. 8. The recovered binding constant K, number of PVP monomers per binding site n, as well as an estimate of the mean number of binding sites per PVP molecule $N = \bar{M}_w/(nM_{\text{mono}})$, where $M_{\text{mono}} = 111$ is the molecular weight of the PVP monomer, are presented in Table 4.

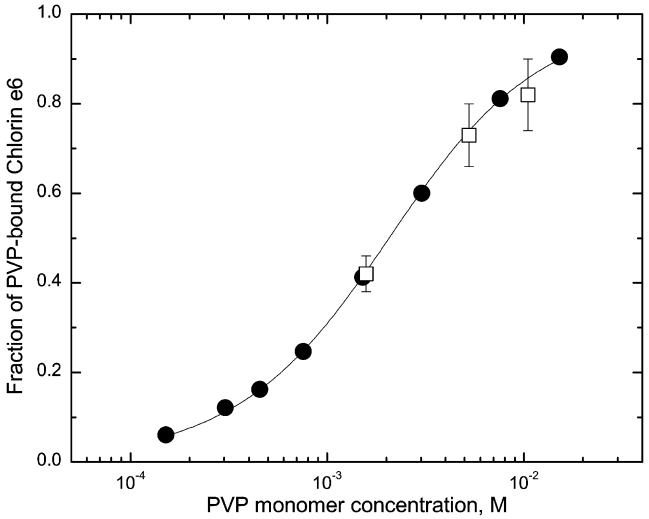

Fig. 8. Fraction of PVP-bound Ce6 ([Ce6] = 1.4×10^{-5} M) as a function of the concentration of PVP K19 (solid circles) and its fit using Eq. (2) (curve). For comparison, the relative contribution of the slow component a_2 of the triplet–triplet absorption of Ce6 as a function of the PVP K19 monomer concentration is overlaid (open squares).

Table 4
Binding parameters of Ce6 with PVP of different molecular weights

Sample	$\bar{M}_W$	K, 10^4 M^{-1}	n	N
PVP K15	8200	3.8 ± 0.6	62 ± 7	1.2 ± 0.1
PVP K19	11,700	3.7 ± 0.6	61 ± 7	1.7 ± 0.2
PVP K30	41,800	3.4 ± 0.5	47 ± 6	8.0 ± 1.0

Note. $\bar{M}_w$ is the PVP weight-average molecular weight of PVP, K is the Ce6–PVP binding constant, n is the number of PVP monomers per binding site, N is the estimate of the mean number of binding sites per PVP molecule. The reported errors of the parameters are the error estimates provided by the non-linear least-squares fitting routine.

The fact that the Ce6–PVP binding constant is virtually independent of the polymer molecular weight, suggests the same binding mechanism for all PVP samples. In this case one should also expect that the number of monomers per binding site should also be independent of M_W. Our measurements, however, show that n drops by about 25% for PVP K30 compared to PVP K15 and PVP K19. This apparent discrepancy can be easily explained by recalling that the polymer samples used in the present study are strongly polydisperse (Table 1), and taking into account that the binding efficiency of PVP drops sharply when its polymerization degree becomes smaller than the number of monomers per binding site [9]. Whereas for PVP K30 the fraction of polymer molecules with the polymerization degree lower than ~50 is negligible, for PVP K15 and PVP K19 this fraction can amount ca. 20–30% of the polymer content. Thus, while the measurements with PVP K30 provide an estimate of n close to its 'real' value, the experiments with shorter polymers PVP K15 and PVP K19 in fact yield 'effective' values of n distorted by the polymer polydispersity.

Therefore, it might seem that PVP K30 is a more favorable choice for as a Ce6 carrier. However, the medical applications impose certain restrictions on the molecular weight of the polymer. Since PVP is not biodegradable and therefore has to be excreted through renal blood vessels, its use in compositions for systemic administration should be restricted to $\bar{M}_w$ below $(5–8) \times 10^4$ (see, e.g. [45]). Therefore, taking into account that the measured $\bar{M}_w$ of 5% of high-molecular fractions of PVP K30 extends far beyond the acceptable range (Table 1), its application for systemic administration is absolutely ruled out due to problems with

elimination of high-molecular weight molecules. At the same time, PVP K19 with the $\bar{M}_w$ of 5% of high-molecular fractions just below the border of the admissible range, appears to be the favorable choice for a Ce6 carrier for systemic administration of the Ce6–PVP formulation.

3.5. Octanol–water partition coefficient

The results of the present study indicate that the changes introduced by PVP into the Ce6 microenvironment can modify the photosensitizer behavior in solution. As a result, PVP can influence the delivery of the photosensitizer to and its localization in the target tissue. In relation to biological systems, it is even more interesting to evaluate how PVP affects the hydrophilic–lipophilic properties of Ce6 and its ability to interact with blood plasma components.

The apparent effect of PVP on hydrophilic–lipophilic properties of Ce6 was evaluated by studying the change in the octanol–water partition coefficient $D_{o/w}$. For Ce6 alone and Ce6–PVP complexes at the Ce6:PVP ratios of 1:10 and 1:100 w/w, the measured partition coefficients $D_{o/w}$ were 1.68 ± 0.06, 0.78 ± 0.07, and 0.49 ± 0.09, respectively (Fig. 9). Thus, the interaction with PVP reduces the octanol–water partition coefficient with an increase in the polymer content. This implies a higher solubility of the polymer-bound photosensitizer in an aqueous phase. Generally, it is expected that an increase in the polarity of the photosensitizer is favorable to its better accumulation in the stroma of the tumor tissue, in which case the photosensitizer causes mainly vascular damage which can be as effective for tumor eradication as the intracellular PDT action [2]. One might speculate that this could as well be the case for the Ce6–PVP complex. To find out, however, what is the real picture, the corresponding *in vivo* experiments are required.

3.6. General discussion

Thus, the results obtained in the present work show that complexation of Ce6 with PVP modifies a number of photophysical and physico-chemical parameters of Ce6. So, is it possible, based on the experimental evidence obtained in the present work to obtain an unambiguous explanation of the enhanced photodynamic activity of Ce6–PVP formulations compared to Ce6 alone?

The photophysical parameters undeniably comprise one of the key factors controlling the efficacy of a PDT drug and a favorable change in photophysics can indeed affect the performance of a PDT formulation. However, our experiments show that the modification of the photophysical properties of Ce6 upon its binding to PVP is far from being dramatic and cannot lead to a substantial enhancement of the PDT efficacy of Ce6–PVP formulations.

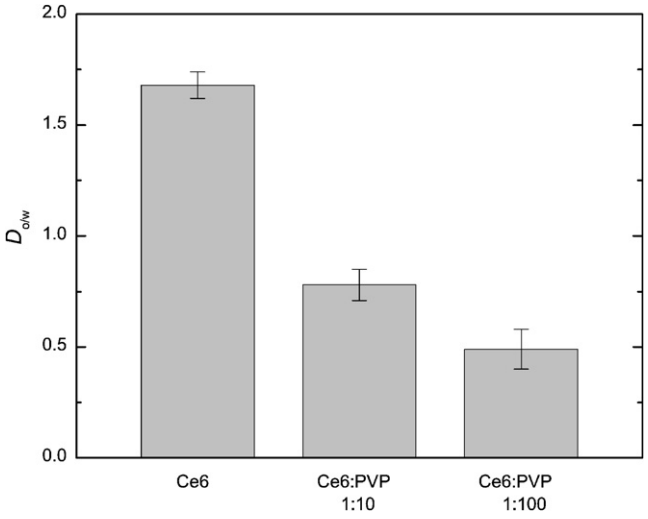

Fig. 9. Octanol–water partition coefficients of Ce6 in the absence of PVP and in the presence of PVP at Ce6:PVP = 1:10 and Ce6:PVP = 1:100.

The aggregation state of a photosensitizing agent can also strongly affect the PDT efficacy of the formulation. In the present work, we have observed that PVP prevents aggregation of Ce6 molecules at lower pH, which can potentially enhance the PDT activity of the formulation. Previous spectroscopic investigations have demonstrated that Ce6 stays predominantly in the monomeric form both in the whole blood [24] and upon cellular uptake [41] at neutral pH. However, to the best of our knowledge, no similar experiments were carried out to study the aggregation state of Ce6 in tumor tissues with a lower-pH environment which may induce Ce6 aggregation. In this case, the disaggregating effect of PVP should enhance the PDT efficacy of a Ce6–PVP formulation compared to Ce6 alone. To elucidate this issue, a comparative study of the Ce6 aggregation state in tumor cells upon uptake of Ce6 and Ce6–PVP-based photosensitizer should be carried out using, e.g., fluorescence lifetime imaging microscopy with picosecond time resolution and subcellular spatial resolution [46].

It is important to point out that in case of the Ce6–PVP formulation with PVP of $M_W = 1.2 \times 10^4$ and Ce6:PVP = 1:1 w/w (Photolon®, Fotolon®), the fraction of PVP-bound Ce6 molecules comprises just a few percent (Fig. 8). Thus, the favorable modification of the PDT parameters of Ce6 molecules bound to PVP could explain the overall enhanced PDT efficacy of Photolon® (Fotolon®) only if one assumes that the overall PDT efficacy of Ce6 alone is extremely low, which is in contradiction with the currently accepted understanding. On the other hand, our *in vivo* experiments have shown that formulations with a higher PVP content (e.g., Ce6:PVP = 1:10) exhibit substantially better tumor/normal tissue contrast and considerably higher tumor necrosis levels (unpublished data, see also [23]). This implies that, rather than directly affecting the PDT activity of the bound photosensitizer, PVP most likely modifies the way Ce6 interacts with the endogenous carriers and distributes between the normal and tumor tissues.

Previously, it has been shown that upon an intravenous administration of Ce6, its transport involves endogenous carrier molecules, in particular, human serum albumin (HSA) and, to a lower extent, low-density lipoproteins (LDL). The corresponding binding constants were estimated as $1.8 \times 10^8\ M^{-1}$ (Ce6–HSA) and $5.7 \times 10^7\ M^{-1}$ (Ce6–LDL) at pH 7.4 [36]. Additionally, lower-affinity Ce6 binding sites in HSA were reported with the binding constant of $1.4 \times 10^6\ M^{-1}$ [34]. The concentration of HSA and LDL in blood are ~40 g/L (597 μM) and ~5.5 g/L (~2 μM), respectively, whereas the concentration of PVP upon intravenous administration of the Ce6–PVP formulation with $M_w = 1.2 \times 10^4$ and Ce6:PVP = 1:1 w/w (Photolon®, Fotolon®) does not exceed 0.04 g/L (~3 μM). The Ce6–PVP binding constant determined in the present paper ($3.7 \times 10^4\ M^{-1}$) is more than two orders of magnitude lower compared to the ones in case of the endogenous carriers. This means that redistribution of Ce6 from PVP to HSA and LDL should take place. In case of a fast redistribution, HSA should serve as a main carrier, and the pharmacokinetic parameters of Ce6 in this case should remind those of free Ce6 [15]. However, animal experiments have shown that the rate of elimination of Ce6 from the tumor tissue is substantially lower in case of Ce6–PVP [20,22]. Additionally, the tumor/normal tissue contrast level is increased several times when Ce6–PVP formulations with a higher content of PVP are used [17]. Therefore, a fraction of Ce6 most likely reaches the tumor either still as a Ce6–PVP complex or, as we speculate, as a ternary Ce6–PVP–HSA complex formed in the bloodstream upon administration of the formulation. Indeed, some experimental results suggest [47] that PVP is able to improve binding of certain compounds by participating in formation of multicomponent complexes. As a result, the hypothetical

Ce6–PVP–HSA complex may have better chances to reach the tumor and reside there for a longer time owing to the enhanced permeability and retention effect [48].

Thus, the results obtained in our study do not offer a clear simple explanation of the improved PDT efficiency of Ce6 non-covalently bound to the PVP polymer carrier, and further investigations are necessary to clarify this issue. In particular, additional experiments are required to find out whether the Ce6–PVP complex is preserved upon its *in vivo* administration and what is the particular mechanism of accumulation and PDT action of Ce6–PVP formulation in tumor.

4. Conclusions

In the present work, in order to gain a better understanding of the high photodynamic efficacy of formulations based on the Ce6–PVP complex, we studied the complexation of Ce6 with PVP at pH values typical for normal and tumor tissues, as well as the effect of the PVP polymer on the photophysical properties of Ce6.

We have demonstrated that Ce6 interacts with PVP in aqueous solution to form molecular complexes with polymer molecules, and established the Ce6–PVP binding constant and the number of monomers per binding site for a range of molecular masses of PVP. We have found that the interaction of Ce6 with PVP prevents Ce6 aggregation and even possibly leads to disruption of already existing aggregates, prevents hydrolysis of Ce6 salts, as well as improves solubility of more hydrophobic mono- and diethyl ethers of Ce6 in the aqueous phase. At the same time, our photophysical experiments with solutions of Ce6 and Ce6–PVP show that PVP-bound Ce6 molecules exhibit an increased fluorescence quantum yield and a virtually unchanged quantum yield of intersystem crossing. These findings, along with our results on Ce6–PVP binding, clearly rule out the possibility that the enhanced photodynamic activity of Ce6–PVP formulation in comparison with Ce6 alone is related to the favorable modification of the photophysical properties of Ce6 in the presence of the polymer.

Though our findings show that at present no clear simple explanation of the enhanced photodynamic efficacy of Ce6–PVP-based formulations can be offered, we speculate that this enhancement can take place due to the disaggregating effect of PVP, as well as due to specific mechanisms of Ce6–PVP interaction with proteins and lipoproteins affecting the Ce6 transport and its distribution in tissues.

5. Abbreviations

Ce6	chlorin e6
PVP	polyvinylpyrrolidone
PDT	photodynamic therapy
HSA	human serum albumin
LDL	low-density lipoprotein

Acknowledgement

The authors are grateful to Mr. A. Panarin for his excellent technical assistance with time-resolved absorption measurements.

References

[1] E.S. Nyman, P.H. Hynninen, Research advances in use of tetrapyrrolic photosensitizers for photodynamic therapy, J. Photochem. Photobiol. B 73 (2004) 1–28.
[2] J. Osterloh, M.G.H. Vicente, Mechanisms of porphyrinoid localization in tumors, J. Porph. Phthaloc. 6 (2002) 305–324.
[3] H. Ringsdorf, Structure and properties of pharmacologically active polymers, J. Polym. Sci. Polym. Symp. 51 (1975) 135–153.
[4] Y.N. Konan, R. Gurny, E. Allemann, State of the art in the delivery of photosensitizers for photodynamic therapy, J. Photochem. Photobiol. B 66 (2002) 89–106.
[5] R. Bachor, C.R. Shea, R. Gillies, T. Hasan, Photosensitized destruction of human bladder carcinoma cells treated with chlorin e6 conjugated microspheres, Proc. Natl. Acad. Sci. USA 88 (1991) 1580–1584.
[6] T.V. Akhlynina, A.A. Rosenkranz, D.A. Jans, A.S. Sobolev, Insulin-mediated intracellular targeting enhances the photodynamic activity of chlorin e6, Cancer Res. 55 (1995) 1014–1019.
[7] M.R. Hamblin, J.L. Miller, I. Rizvi, B. Ortel, E.V. Maytin, T. Hasan, Pegylation of chlorin e6 polymer conjugate increases tumor targeting of photosensitizer, Cancer Res. 61 (2001) 7155–7162.
[8] S.I. Ogura, Y. Fujita, T. Kamachi, C. Okura, Preparation of chlorin e6-monoclonal antibody conjugate and its effect for photodynamic therapy, J. Porph. Phthaloc. B 5 (2001) 486–489.
[9] Yu.E. Kirsh, Poly-*N*-Vinylpyrrolidone and Other Poly-*N*-Vinylamides: Synthesis and Physico-Chemical Properties, Nauka, Moscow, 1998. (in Russian).
[10] A. Kubin, L.H. Guenter, Novel preparation hypericin bonded poly-*N*-vinylamides, European patent EP1289562, 2003.
[11] Y. Kaneda, Y. Tsutsumi, Y. Yoshioka, H. Kamada, Y. Yamamoto, H. Kodaira, S. Tsunoda, T. Okamoto, Y. Mukai, H. Shibata, S. Nakagawa, T. Mayumi, The use of PVP as a polymeric carrier to improve the plasma half-life of drugs, Biomaterials 25 (2004) 3259–3266.
[12] H. Kamada, Y. Tsutsumi, S. Tsunoda, T. Kihira, Y. Kaneda, Y. Yamamoto, S. Nakagawa, Y. Horisawa, T. Mayumi, Molecular design of conjugated tumor necrosis factor-alpha: synthesis and characteristics of polyvinyl pyrrolidone modified tumor necrosis factor-alpha, Biochem. Biophys. Res. Commun. 257 (1999) 448–453.
[13] I.G. Savkina, V.B. Evstigneev, Photochemical properties of water soluble chlorophyll analogs in free and bound state, Biokhimia 9 (1964) 975–981. (in Russian).
[14] H. Kamada, Y. Tsutsumi, Y. Yamamoto, T. Kihira, Y. Kaneda, Y. Mu, H. Kodaira, S. Tsunoda, S. Nakagawa, T. Mayumi, Antitumor activity of tumor necrosis factor-alpha conjugated with polyvinylpyrrolidone on solid tumors in mice, Cancer Res. 60 (2000) 6416–6420.
[15] G.A. Kostenich, I.N. Zhuravkin, E.A. Zhavrid, Experimental grounds for using chlorin e6 in the photodynamic therapy of malignant tumors, J. Photochem. Photobiol. B 22 (1994) 211–217.
[16] P.T. Petrov, V.M. Tsarenkov, A.P. Meshcheryakova, O.N. Albitskaya, V.I. Tyurin, M.P. Sarzhevskaya, A.D. Kochubeeva, I.N. Zhuravkin, Agent for photodynamic treatment of malignant tumors – photolon, Republic of Belarus Patent No. 5651, 1999.
[17] P. Petrov, T. Trukhacheva, H. Isakau, M. Haurylau, M. Kaplan, Mittel für die photodynamische Diagnostik und Therapie von bösartigen Tumoren, German Patent Application DE10316566, 2003.
[18] P.T. Petrov, T.V. Trukhacheva, G.A. Isakov, S.V. Shlyakhtin, L.N. Marchenko, Yu.P. Istomin, Photolon, a remedy for photodynamic therapy and diagnosis: Clinical experience, Vestnik Farmatsii 3 (37) (2007) 69–81. (in Russian).
[19] W.L.L. Chin, W.K.O. Lau, R. Bhuvaneswari, P.W.S. Heng, M. Olivo, Chlorin e6-polyvinylpyrrolidone as a fluorescent marker for fluorescence diagnosis of human bladder cancer implanted on the chick chorioallantoic membrane model, Cancer Lett. 245 (2007) 127–133.
[20] W.W.L. Chin, P.W.S. Heng, R. Bhuvaneswari, W.K.O. Lau, M. Olivo, The potential application of chlorin e6–polyvinylpyrrolidone formulation in photodynamic therapy, Photochem. Photobiol. Sci. 5 (2006) 1031–1037.
[21] W.W.L. Chin, W.K.O. Lau, P.W.S. Heng, R. Bhuvaneswari, M. Olivo, Fluorescence imaging and phototoxicity effects of new formulation of chlorin e6–polyvinylpyrrolidone, J. Photochem. Photobiol. B 84 (2006) 103–110.
[22] Fotolon®: Nonclinical Summary (Synopsis), RUE Belmedpreparaty, Minsk, 2003; or Fotolon™: Nonclinical Summary (Synopsis). HAEMATO-science GmbH, Germany. Version: 5.10.2003.
[23] P.T. Petrov, H.A. Isakau, T.V. Trukhacheva, M.V. Haurylau, M.A. Kaplan, Agent for photodynamic diagnosis and treatment of oncological diseases, International Patent Application WO2004110438, 2004.
[24] M.V. Parkhots, V.N. Knyukshto, G.A. Isakov, P.T. Petrov, S.V. Lepeshkevich, A.Ya. Khairullina, B.M. Dzhagarov, Spectral-luminescent studies of the photosensitizer "Photolon" in the model systems and in blood of oncological patients, J. Appl. Spectrosc. 70 (2003) 921–926.
[25] L.E. Gerweck, K. Seetharaman, Cellular pH gradient in tumor versus normal tissue: potential exploitation for the treatment of cancer, Cancer Res. 56 (1996) 1194–1198.
[26] B. Čunderlíková, L. Gangeskar, J. Moan, Acid–base properties of chlorin e6: relation to cellular uptake, J. Photochem. Photobiol. B 53 (1999) 81–90.
[27] S. Lötjönen, P.H. Hynninen, A convenient method for the preparation of chlorin e6 and rhodin g7 trimethyl esters, Synthesis 7 (1980) 541–543.
[28] H.A. Isakau, T.V. Trukhacheva, A.I. Zhebentyaev, P.T. Petrov, HPLC study of chlorin e6 and its molecular complex with polyvinylpyrrolidone, Biomed. Chromatogr. 21 (2007) 318–325.
[29] H.A. Isakau, T.V. Trukhacheva, P.T. Petrov, Isolation and identification of impurities in chlorin e6, J. Pharm. Biomed. Anal. 45 (2007) 20–29.
[30] L. Bourre, G. Simonneaux, Y. Ferrand, S. Thibaut, Y. Lajat, T. Patrice, Synthesis, and in vitro and in vivo evaluation of a diphenylchlorin sensitizer for photodynamic therapy, J. Photochem. Photobiol. B 69 (2003) 179–192.
[31] E. Zenkevich, E. Sagun, V. Knyukshto, A. Shulga, A. Mironov, O. Efremova, R. Bonnett, S.P. Songca, M. Kassem, Photophysical and photochemical properties

of potential porphyrin and chlorin photosensitizers for PDT, J. Photochem. Photobiol. B 33 (1996) 171–180.
[32] D.V. O'Connor, D. Phillips, Time-Correlated Single Photon Counting, Academic Press, London, 1984.
[33] J.C. Scaiano, Nanosecond laser flash photolysis: a tool for physical organic chemistry, in: R.A. Moss, M.S. Platz, M. Jones Jr. (Eds.), Reactive Intermediate Chemistry, John Wiley and Sons, Hoboken, NJ, 2004, pp. 847–871.
[34] G.A. Kochubeev, A.A. Frolov, E.E. Zenkevich, G.P. Gurinovich, Regularities of complex formation of chlorin e6 with human and bovine serum albumins, Mol. Biol. 22 (1988) 774–780.
[35] A.A. Frolov, E.I. Zenkevich, G.P. Gurinovich, G.A. Kochubeev, Chlorin e6–liposome interaction. Investigation by the methods of fluorescence spectroscopy and inductive resonance energy transfer, J. Photochem. Photobiol. B 7 (1990) 43–56.
[36] H. Mojzisova, S. Bonneau, C. Vever-Bizet, D. Brault, The pH-dependent distribution of the photosensitizer chlorin e6 among plasma proteins and membranes: a physico-chemical approach, Biochim. Biophys. Acta 1768 (2007) 366–374.
[37] B.M. Dzhagarov, E.I. Sagun, V.A. Ganzha, G.P. Gurinovich, The mechanism of quenching the triplet state of chlorophyll and related compounds by molecular oxygen, Sov. J. Chem. Phys. 6 (1990) 1784–1807.
[38] E.I. Zenkevich, G.A. Kochubeev, K.I. Salokhiddinov, Spectral-luminescent and energy characteristics of water-soluble chlorin pigment bound to a protein carrier, J. Appl. Spectrosc. 29 (1978) 1198–1203.
[39] A.A. Frolov, G.A. Kochubeev, G.P. Gurinovich, Photodynamic effect of chlorin e6 on biological systems, Studia Biophys. 134 (1989) 235–247.
[40] V.Yu. Plavskii, V.A. Mostovnikov, G.R. Mostovnikova, A.I. Tretyakova, L.G. Plavskaya, Regularities of bonding of chlorin e6 on the oligomeric enzyme lactate dehydrogenase, J. Appl. Spectrosc. 70 (2003) 913–920.
[41] A.A. Frolov, Yu.M. Arkatov, G.P. Gurinovich, G.A. Kochubeev, M.V. Sarzhevskaya, S.N. Cherenkevich, Intracellular localization of exogenic photosensitizer – chlorin e6, Dokl. Akad. Nauk. SSSR 291 (1986) 715–719. (in Russian).
[42] G. Van den Mooter, P. Augustijns, N. Blaton, R. Kinget, Physico-chemical characterization of solid dispersions of temazepam with polyethylene glycol 6000 and PVP K30, Int. J. Pharm. 164 (1998) 67–80.
[43] A.B. Uzdensky, D.E. Bragin, M.S. Kolosov, A. Kubin, H.G. Loew, J. Moan, Photodynamic effect of hypericin and a water-soluble derivative on isolated crayfish neuron and surrounding glial cells, J. Photochem. Photobiol. B 72 (2003) 27–33.
[44] C.R. Cantor, P.R. Schimmel, Biophysical Chemistry. Part III: The Behavior of Biological Macromolecules, W.H. Freeman & Co., 1980.
[45] B.V. Robinson, F.M. Sullivan, J.F. Borzelleca, S.L. Schwartz, PVP: A Critical Review of the Kinetics and Toxicology of Polyvinylpyrrolidone (Povidone), Lewis Publishers, Chelsea, MI, 1990.
[46] L. Kelbauskas, W. Dietel, Internalization of aggregated photosensitizers by tumor cells: Subcellular time-resolved fluorescence spectroscopy on derivatives of pyropheophorbide-a ethers and chlorin e6 under femtosecond one- and two-photon excitation, Photochem. Photobiol. 76 (2002) 686–694.
[47] R. Chadha, D.V.S. Jain, A. Aggarwal, S. Singh, D. Thakur, Binding constants of inclusion complexes of nitroimidazoles with β-cyclodextrins in the absence and presence of PVP, Thermochim. Acta 459 (2007) 111–115.
[48] H. Maeda, T. Sawa, T. Konno, Mechanism of tumor-targeted delivery of macromolecular drugs, including the EPR effect in solid tumor and clinical overview of the prototype polymeric drug SMANCS, J. Control Release 74 (2001) 47–61.